Photochemical reaction of $W(CO)_6$ with $SnCl_4$
I. Synthesis and X-ray structure
of tri-μ-chloro-trichlorostannate-heptacarbonylditungsten(II)
$[(CO)_4W(\mu\text{-}Cl)_3W(SnCl_3)(CO)_3]$

Teresa Szymańska-Buzar *, Tadeusz Głowiak

Institute of Chemistry, University of Wrocław, 50-383 Wrocław, Poland

Abstract

The crystal structure of $[(CO)_4W(\mu\text{-}Cl)_3W(SnCl_3)(CO)_3]$ (1) formed in the photochemical reaction of $W(CO)_6$ with $SnCl_4$ was determined by the single-crystal X-ray diffraction method. The crystals are orthorhombic, of space group *Pbca*, $a = 12.706(3)$ Å, $b = 16.655(4)$ Å, $c = 18.669(3)$ Å, $V = 3951(2)$ Å^3 and $Z = 8$. The structure solved by the heavy-atom method has been refined to $R = 0.0299$ for 2187 observed reflections. The tungsten atoms in the molecule are both seven-coordinate, each being bonded to three bridging chlorines, to four CO groups on one end and three CO groups and a $SnCl_3$ group on the other. For each tungsten, there is a 4-3 geometry of ligand. Nuclear magnetic resonance, IR and electronic absorption spectroscopies were used to examine the title compound. Compound 1 is a unique example of the halo carbonyls of Group 6 metals with an M–Sn bond.

Keywords: Tungsten; Tin; Carbonyl; Heterobimetallic; Crystal structure; Oxidative addition

1. Introduction

Lewis acids are often associated with transition metal derivatives to promote both stoichiometric and catalytic reactions. This is the case for the metathesis and isomerization reactions of olefins [1–4], for the polymerization reaction of alkynes [5] and CO insertion reaction into metal alkyl derivatives [6]. It has been shown in these cases that the Lewis acid strongly interacts with the oxygen atom of a coordinated CO group [1–6].

The role of Lewis acids in a catalytic system containing $M(CO)_6$ (M = W or Mo) is connected rather with the labilization effect of the CO group and its very fast substitution by alkene or alkyne [1–5,7].

In the course of our studies on catalytic activity of Group 6 metal carbonyls activated by metal or nonmetal halides (Lewis acids), we have tried to explain the role of CCl_4 [1,2], $ZrCl_4$ [1–5] and also $SnCl_4$ in the formation of a catalytic intermediate for transformation of alkenes [1–3] or alkynes [5,7].

Previous reports have indicated that photolysis of tungsten hexacarbonyl in cyclohexane in the presence of CCl_4 yields product formulated as $[W(CO)_4Cl_2]_2$ [1,8,9]. In order to pursue this reaction type further, we undertook studies of the photochemical reaction of the $W(CO)_6$ with $SnCl_4$ to determine whether new W^{II} complexes might be obtained in a reaction analogous to those above. The results of these studies are described below.

2. Results and discussion

There have been studies of the action of SnR_nX_{4-n} on Group 6 M^0 carbonyls substituted by bidentate chelating ligands L–L containing nitrogen [10–15], phosphorus [10], or sulfur donors [12b]. Thus, the oxidation addition reaction of $[M(CO)_4L\text{-}L]$ with $SnR_n\text{-}X_{4-n}$ gives monomeric seven-coordinate M^{II} (M = Mo or W) compounds $[MX(SnR_nX_{3-n})(CO)_3(L\text{-}L)]$ con-

* Corresponding author.

taining M–Sn bonds, with the loss of one molecule of carbon monoxide. Recently, Baker and co-workers reported the oxidation addition of $SnCl_4$ to $[M(CO)_3(NCMe)_3]$ to give $[MCl(SnCl_3)(CO)_3(CNMe)_2]$ in which the labile acetonitrile ligands can be replaced by others [16,17]. Miguel et al. [18] and Cano et al. [19] have explored the reactions of $[M(CO)_3(nitrile)_3]$ with haloalkyltin derivatives SnR_nCl_{4-n}.

Our work has led to the discovery and structural characterization of a new binuclear tungsten tin chloro carbonyl compound, $[(CO)_4W(\mu\text{-}Cl)_3W(SnCl_3)(CO)_3]$ (1). Neither this compound nor any other $[M_2X_3\text{-}(SnX_3)(CO)_7]$ compound has previously been reported.

### 2.1. Photochemical reaction of $W(CO)_6$ with $SnCl_4$

Irradiation of $W(CO)_6$ in cyclohexane with an equimolar amount of $SnCl_4$ results in the immediate formation of a deep yellow solution, and then an orange precipitate. The IR spectrum of the reaction mixture shows the decay of the band at 1980 cm^{-1}; this is attributable to $W(CO)_6$ and the appearance of a very low intensity band at 2100, 2020 and 1942 cm^{-1} (broad) characteristic of the oxidation reaction product $[(CO)_4W(\mu\text{-}Cl)_3W(SnCl_3)(CO)_3]$ (1), which is almost quantitatively precipitated from the reaction mixture. The complex is air-sensitive in the solid state and extremely air-sensitive in solution, but it can be stored under nitrogen in the solid state for months. Complex 1 is only slightly soluble in aliphatic hydrocarbons but considerably more soluble in aromatic solvents and is readily soluble in CH_2Cl_2 or $CHCl_3$.

The formation of complex 1 (Eq. (1)) is a typical oxidative addition reaction of metal carbonyls in which the carbon monoxide ligands are expelled and replaced by two univalent ligands. The formal oxidation state of the metal increases by 2 units:

$$2W(CO)_6 + 2SnCl_4$$
$$\xrightarrow[C_6H_{12}]{h\nu} [(CO)_4W(\mu\text{-}Cl)_3W(SnCl_3)(CO)_3]$$
$$+ 5CO + SnCl_2 \qquad (1)$$
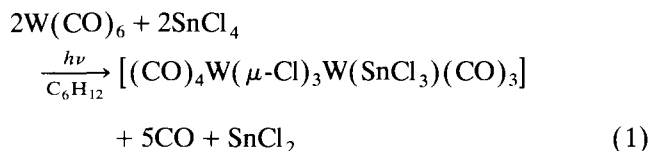
The reaction mechanism for the formation of 1 is not known. However, of the reactions which have occurred, there are precedents for the formation of $[W(CO)_4CL_2]_2$ from the photochemical reaction of tungsten hexacarbonyl with CCl_4 [1,8,9]. The oxidative addition reaction of $M(CO)_6$ (M = W, Mo, Cr) with CCl_4 is initiated by an electron transfer from $M(CO)_6$ to the CCl_4, which can be regarded as an electron acceptor, to produce the anion radical, CCl_4^- (Eq. (2)) [1]:

$$M(CO)_6 + CCl_4 \xrightarrow{h\nu} [M(CO)_6^+ \ldots CCl_4^-]$$
$$\rightarrow [M(CO)_5Cl] + \cdot CCl_3 + CO, \qquad (2)$$
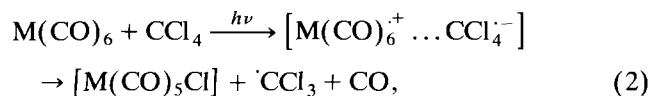
Secondly, CCl_4^- may decompose to give a $\cdot CCl_3$ radical and Cl^- ions which then serve to stabilize the oxidized paramagnetic metal system. An attack by $\cdot CCl_3$ on the oxidized metal system leads to the M^{II} and dichlorocarbene species. A compound of M^{II} can also be formed in a disproportionation reaction shown in Eq. (3):

$$2[M(CO)_5Cl] \longrightarrow M(CO)_6 + [M(CO)_4Cl_2] \qquad (3)$$
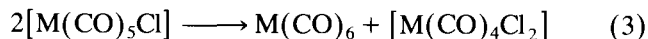
It seems very probable that in the formation of compound 1, similar free-radical intermediates may be involved with $SnCl_4$ serving as a source of chlorine, elision of $SnCl_2$ and $[W(CO)_4Cl_2]$ appearance. Photochemical oxidation addition of $W(CO)_6$ with $SnCl_4$ and formation of a W–Sn bond can occur in parallel (Eq. (4)):

$$W(CO)_6 + SnCl_4 \xrightarrow{h\nu} [WCl(SnCl_3)(CO)_4] + 2CO \qquad (4)$$
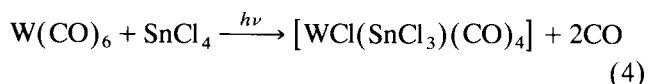
The dimerization of these two W^{II} compound with the elimination of CO gave complex 1 (Eq. 5):

$$[W(CO)_4Cl_2] + [WCl(SnCl_3)(CO)_4]$$
$$\longrightarrow [(CO)_4W(\mu\text{-}Cl)_3W(SnCl_3)(CO)_3] + CO \qquad (5)$$
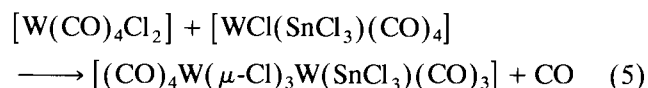
The complex 1 was fully characterized by elemental analysis (C,Cl,Sn), IR and ^{13}C NMR spectroscopy and also mass spectrometric investigation (see Section 3). Unfortunately under standard conditions (electron impact and evaporation from a crucible), the compound
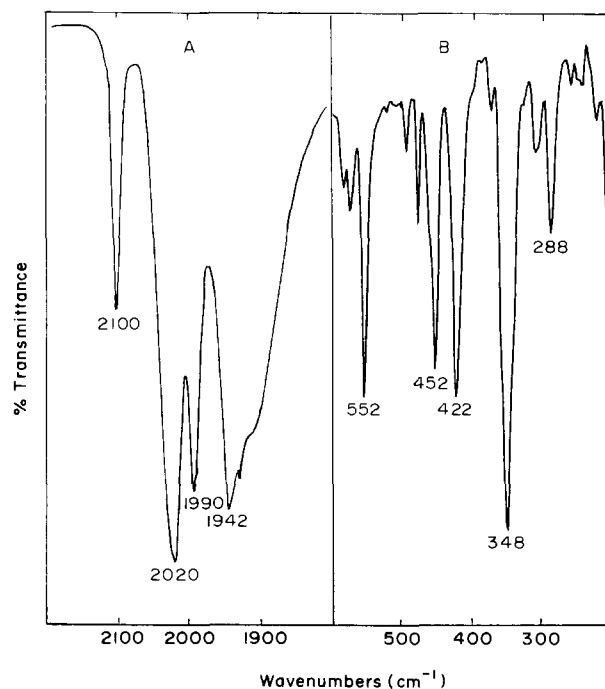

Fig. 1. (A) ν(CO) region of the IR absorption spectrum displayed by complexes $[(CO)_4W(\mu\text{-}Cl)_3W(SnCl_3)(CO)_3](1)$ in KBr. (B) ν(SnCl) region of the IR absorption spectrum of 1 in Nujol mulls

decomposes. A soft ionization method such as fast atom bombardment in sulfolane S as matrix material shows a reaction product of S with compound 1. Although these results do not allow conclusions concerning the nature of compound 1, they indicate its high reactivity.

The IR spectrum of $[(CO)_4W(\mu - Cl)_3W(SnCl_3)(CO)_3]$ (1) in KBr containing four well resolved $\nu(CO)$ bands at 2100m, 2020vs, 1990s and 1942s(broad) with shoulders at 1924 and 1910 cm^{-1} (Fig. 1A). The energies of these bands suggest the formation of the W^{II} compound; indeed, the spectrum resembles quite closely that of $[WCl_2(CO)_4]_2$ (νCO in C_6H_{12}: 2100w, 2010s and 1940m cm^{-1} [8], νCO in KBr: 2100m, 2014s, 1988s, and 1939m cm^{-1} [20]), $[WBr_2(CO)_4]_2$ (νCO in CH_2Cl_2: 2095w, 2020s and 1935m cm^{-1} [21]), and $[W_2Br_2(CO)_7]$ (νCO in CH_2Cl_2: 2110w, 2100w, 2050m, 2038s, 2025s, 1974m, and 1950m cm^{-1} [21].

The spectrum of 1 is in good accord with the structure, which consists of two non-equivalent halves, $W(CO)_4$ and $W(CO)_3$.

The low frequency region of the infrared spectrum of 1 is dominated by a principal absorption at 348s cm^{-1} (Fig. 1B), which can be regarded as $\nu_{sym.}$ Sn–Cl vibration; $\nu_{asym.}$ Sn–Cl vibration is most probably at 288 cm^{-1}. There has been a great deal of confusion in the literature about the correct assignment of tin–halide frequencies of the SnCl$_3^-$ ligand [38], and also on the region of transition metal–halide and other metal-ligand frequencies. In many cases these bands are not resolved. Tin-halide frequencies of [SnCl$_3$]$^-$ were observed in the IR spectrum of [Ph$_4$As][SnCl$_3$] at 291vw, and 258w cm^{-1} [22] and in the spectrum of the tetraethylammonium salts at 280m and 241s cm^{-1} [23]. Such high energy Sn–Cl vibration as in compound 1 was observed only in Mo– or W–Sn complexes of the type [MCl(SnCl$_3$)(CO)$_3$(L–L)] [13,14]. This is in good agreement with increased frequencies of these bands upon coordination to metal or other ligand [24] and shortening of the Sn–Cl bond lengths in compound 1 compared to free SnCl$_3^-$ [25].

The frequency of W–Cl is of lower intensity and energy than Sn–Cl. In tungsten(II) compounds, [WCl$_2$(CO)$_3$(PPh$_3$)$_2$] [8], terminal ν(WCl) vibration is observed at 300 cm^{-1}. A detailed analysis of the spectrum of [W$_2$Cl$_9$]$^{3-}$ [26] has assigned all the bands near 300 cm^{-1} as primarily terminal W–Cl stretching frequencies while the band near 210 cm^{-1} is due to a bridging W–Cl stretching frequency.

The complex is fluxional at room temperature as judged by ^{13}C NMR spectroscopy (Fig. 2). At 243 K, the dynamic process is quenched, giving sharp, well resolved spectra, whose assignment is consistent with the solid state structure. At room temperature, the ^{13}C NMR spectrum of 1 in C$_6$D$_5$CD$_3$ appears as one broad singlet at 204.23 ppm with ^{183}W satellites. At 243 K
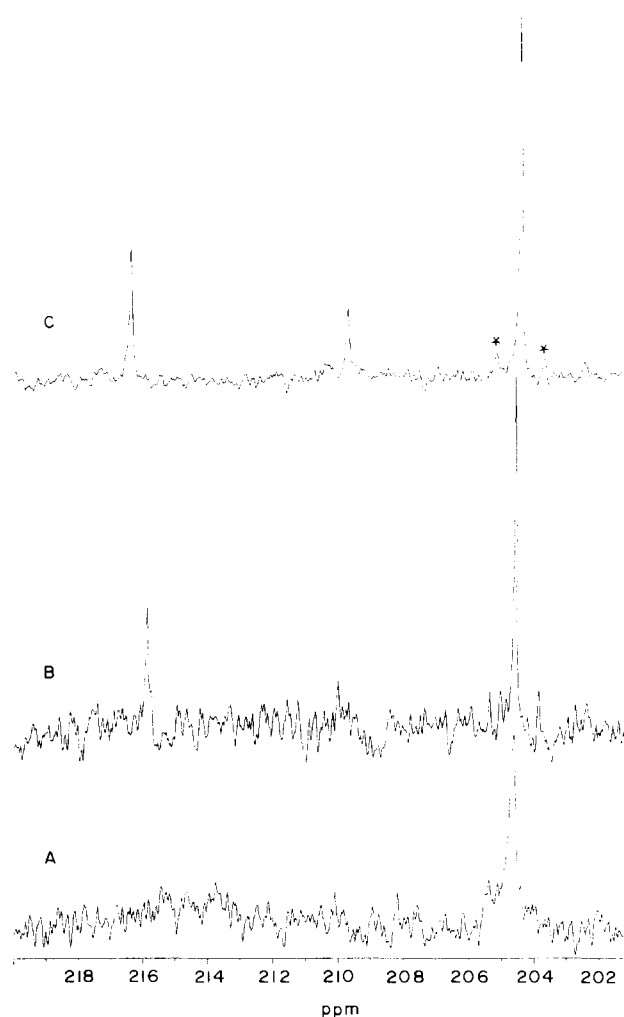

Fig. 2. ^{13}C NMR spectra, recorded at different temperature: (A) 293 K, (B) 243 K, (C) 223 K and 75 MHz with toluene-d_8 as solvent, in the CO carbon region of the sample [(CO)$_4$W(μ-Cl)$_3$W(SnCl$_3$)(CO)$_3$] (1). The resonances denoted by an asterisk arise from coupling to ^{183}W, $I = 1/2$, 14.5% natural abundance.

and at lower temperature (223, 203 and 183 K), the ^{13}C spectrum of compound 1 appears as three singlets at 215.43, 209.60 and 204.23 ppm, which broaden upon warming and two of them disappear to produce a singlet (204.23 ppm) at 293 K. The more intense CO resonance centered at δ 204.23 ppm in the ^{13}C spectrum shows splitting due to ^{183}W–^{13}C coupling with $J = 108$ Hz. The intensity ratio of carbon CO signals at 243 K is 2:1:4 but changes upon cooling. The resonance at higher field (204.23 ppm) is most likely due to four equivalent carbonyl ligands connected to W(1) and resonances at lower field (215.43 and 209.60 ppm) belong to three non-equivalent (2:1) carbonyls bonded to W(2) effectively more oxidized than W(1).

The correlation has been made between carbonyl chemical shift and electron density at the carbon atom which would suggest that for closest metal–carbonyl contact, a larger shift to higher frequency must be
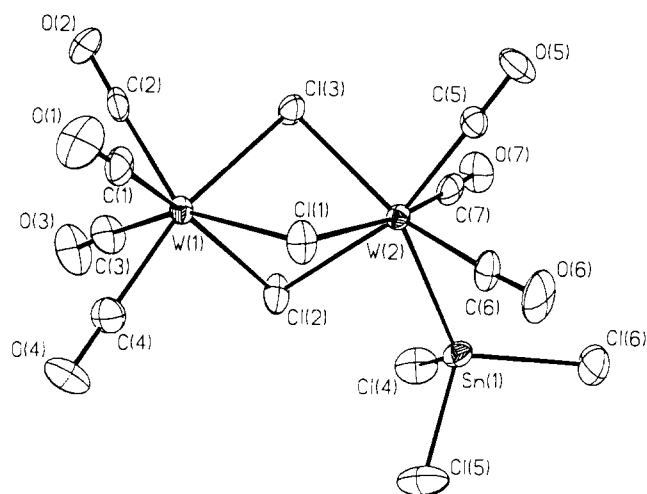
Fig. 3. An ortep [45] view of the [(CO)₄W(μ-Cl)₃W(SnCl₃)(CO)₃] (1) molecule showing the atom numbering scheme used in the tables.

observed [27]. The ^{13}C NMR spectrum of [Mo-(CO)₄Br₃]⁻ consists of two signals at 247.0 and 210.6 ppm of intensities 1:3 consistent with the C_{3v} symmetry of the tungsten analogue in the solid state [28]. The resonance due to the most strongly bond capping carbonyl is at 247.0 ppm.

2.2. Structure of [(CO)₄W(μ − Cl)₃W(SnCl₃)(CO)₃] (1)

The compound **1** is formed of discrete dinuclear unsymmetrical molecules having the structure shown in

Table 1
Final atomic coordinates with e.s.d.s ($\times 10^5$) for W and Sn, ($\times 10^4$) for remaining atoms and equivalent isotropic thermal parameters with e.s.d.s ($\text{Å}^2 \times 10^4$)

Atom	x	y	z	U_{eq} [a]
W(1)	17804(4)	8253(3)	9401(3)	284(1)
W(2)	19253(4)	19038(3)	−6810(3)	281(1)
Sn(1)	35943(7)	16078(6)	−15637(5)	392(2)
Cl(1)	2423(1)	2174(1)	6150(1)	453(8)
Cl(2)	2708(1)	576(1)	−227(1)	586(11)
Cl(3)	461(1)	1265(1)	−2(1)	516(10)
Cl(4)	3575(1)	343(1)	−2094(1)	732(13)
Cl(5)	5242(1)	1620(1)	−1035(1)	820(2)
Cl(6)	3818(1)	2441(1)	−2554(1)	970(2)
O(1)	1367(1)	1702(1)	2408(1)	750(4)
O(2)	−413(1)	231(1)	1524(1)	720(4)
O(3)	1912(1)	−1061(1)	992(1)	830(4)
O(4)	3799(1)	422(1)	1893(1)	880(4)
O(5)	286(1)	3250(1)	−1026(1)	700(3)
O(6)	3193(1)	3495(1)	−866(1)	790(4)
O(7)	1019(1)	1368(1)	−2166(1)	630(3)
C(1)	1492(1)	1393(1)	1883(1)	470(4)
C(2)	378(1)	430(1)	1316(1)	450(4)
C(3)	1842(1)	−400(1)	984(1)	560(4)
C(4)	3082(1)	583(1)	1567(1)	490(4)
C(5)	894(1)	2778(1)	−897(1)	390(3)
C(6)	2780(1)	2895(1)	−837(1)	450(4)
C(7)	1371(1)	1563(1)	−1630(1)	470(4)

[a] $U_{eq} = 1/3 \Sigma_{ij} U_{ij} a_i^* a_j^* \vec{a}_i \vec{a}_j$.

Table 2
Selected bond lengths (Å) and angles (°) with e.s.d.s in parentheses

Bond distances

W(1)–W(2)	3.525(1)	W(1)–C(3)	2.04(1)
W(1)–Cl(1)	2.467(3)	W(1)–C(4)	2.07(2)
W(1)–Cl(2)	2.512(3)	W(2)–C(5)	2.00(1)
W(1)–Cl(3)	2.538(3)	W(2)–C(6)	2.00(1)
W(2)–Cl(3)	2.490(3)	W(2)–C(7)	1.99(2)
W(2)–Cl(1)	2.540(3)	O(1)–C(1)	1.12(2)
W(2)–Cl(2)	2.569(3)	O(2)–C(2)	1.13(2)
W(2)–Sn(1)	2.731(1)	O(3)–C(3)	1.11(2)
Sn(1)–Cl(5)	2.314(4)	O(4)–C(4)	1.13(2)
Sn(1)–Cl(4)	2.327(4)	O(5)–C(5)	1.13(2)
Sn(1)–Cl(6)	2.330(5)	O(6)–C(6)	1.13(2)
W(1)–C(1)	2.03(2)	O(7)–C(7)	1.14(2)
W(1)–C(2)	2.03(2)		

Bond angles

C(2)–W(1)–C(1)	72.1(6)	C(5)–W(2)–Cl(1)	103.0(4)
C(2)–W(1)–C(3)	72.2(6)	C(7)–W(2)–Cl(2)	100.7(4)
C(1)–W(1)–C(3)	115.9(6)	C(6)–W(2)–Cl(2)	123.3(4)
C(2)–W(1)–C(4)	116.4(6)	C(5)–W(2)–Cl(2)	161.3(4)
C(1)–W(1)–C(4)	75.2(6)	Cl(3)–W(2)–Cl(1)	77.1(1)
C(3)–W(1)–C(4)	75.6(6)	Cl(3)–W(2)–Cl(2)	75.7(1)
C(2)–W(1)–Cl(1)	132.3(4)	Cl(1)–W(2)–Cl(2)	75.0(1)
C(1)–W(1)–Cl(1)	81.3(4)	C(7)–W(2)–Sn(1)	71.7(4)
C(3)–W(1)–Cl(1)	155.1(5)	C(6)–W(2)–Sn(1)	68.8(4)
C(4)–W(1)–Cl(1)	93.0(4)	C(5)–W(2)–Sn(1)	121.3(4)
C(2)–W(1)–Cl(2)	131.3(4)	Cl(3)–W(2)–Sn(1)	144.1(1)
C(1)–W(1)–Cl(2)	155.9(4)	Cl(1)–W(2)–Sn(1)	114.4(1)
C(3)–W(1)–Cl(2)	81.5(5)	Cl(2)–W(2)–Sn(1)	75.1(1)
C(4)–W(1)–Cl(2)	94.8(4)	Cl(5)–Sn(1)–Cl(4)	101.5(2)
C(2)–W(1)–Cl(3)	75.7(4)	Cl(5)–Sn(1)–Cl(6)	102.9(2)
C(1)–W(1)–Cl(3)	110.3(4)	Cl(4)–Sn(1)–Cl(6)	101.7(2)
C(3)–W(1)–Cl(3)	110.0(5)	Cl(5)–Sn(1)–W(2)	116.3(1)
C(4)–W(1)–Cl(3)	167.9(4)	Cl(4)–Sn(1)–W(2)	114.3(1)
Cl(1)–W(1)–Cl(2)	77.4(1)	Cl(6)–Sn(1)–W(2)	117.8(1)
Cl(1)–W(1)–Cl(3)	77.6(1)	W(1)–Cl(1)–W(2)	89.5(1)
Cl(2)–W(1)–Cl(3)	75.9(1)	W(1)–Cl(2)–W(2)	87.8(1)
C(7)–W(2)–C(6)	107.3(5)	W(2)–Cl(3)–W(1)	89.0(1)
C(7)–W(2)–C(5)	78.3(6)	O(1)–C(1)–W(1)	178.(2)
C(6)–W(2)–C(5)	74.0(6)	O(2)–C(2)–W(1)	178.(1)
C(7)–W(2)–Cl(3)	93.8(4)	O(3)–C(3)–W(1)	177.(2)
C(6)–W(2)–Cl(3)	146.5(4)	O(4)–C(4)–W(1)	177.(1)
C(5)–W(2)–Cl(3)	85.6(4)	O(5)–C(5)–W(2)	178.(1)
C(7)–W(2)–Cl(1)	170.7(4)	O(6)–C(6)–W(2)	172.(1)
C(6)–W(2)–Cl(1)	81.8(4)	O(7)–C(7)–W(2)	178.(1)

Fig. 3. Table 1 contains the fractional coordinates and isotropic thermal parameters. The bond distances and the important bond angles are given in Table 2.

The basic structural units of **1** are two seven-coordinate tungsten atoms, which are linked by three chlorine atoms occupying a bridging position between the two tungsten atoms.

In this molecule, a coordination number of seven for tungsten(II) atoms is achieved in a different way and results in a different type of coordination polyhedron about the metal atoms. For each tungsten atom there is a 4-3 geometry of ligands, with the set of three for each one being the three chlorine atoms that are shared as μ-Cl bridges. At one end, W(1), the set of four ligands is made up entirely of CO groups while at the other
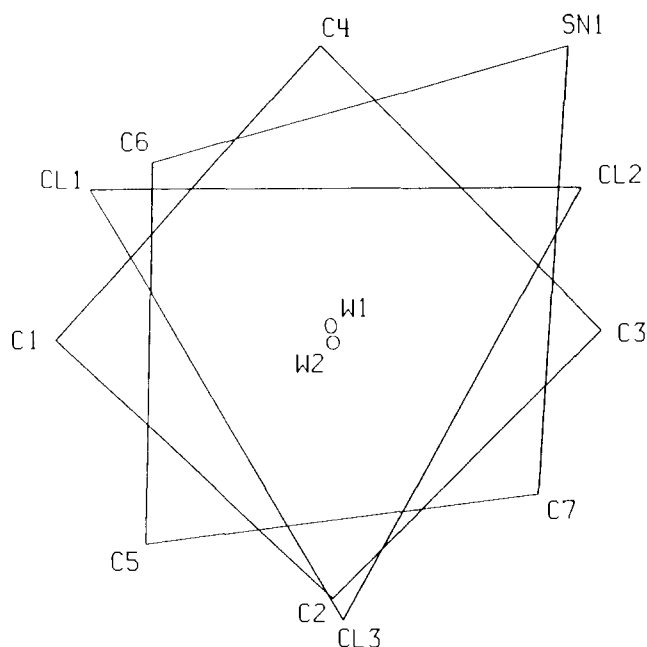
Fig. 4. The coordination sphere of W(1) and W(2) in diagrammatic form. The projection of coordination sphere of W(1) and W(2) in diagrammatic form. The projection of coordination sphere of W(1) and W(2) on the Cl(1)–Cl(2)–Cl(3) plane I. The angle between plane I Cl(1)–Cl(2)–Cl(3) and plane II through C(1)–C(2)–C(3)–C(4) is 1.2(1)°; the angle between plane I and plane III through C(5)–C(6)–C(7)–Sn(1) is 4.7(1)°; the angle between plane II and III is 5.3(1)°.

shown in Fig. 4 which is a projection of the coordination spheres of W(1) and W(2) on the trichloro-bridge, thus illustrating the 4-3 geometry. Both quadrilateral faces are planar and approximately parallel to the triangular face (angle of intersection 1.2(1)° and 4.7(1)°; Fig. 4). In this projection, one chlorine atom of the trigonal base overlaps one carbon atom of the tetragonal base with W(1) in the center. None of the atoms in the W(2) quadrilateral base overlap atoms of the trigonal plane.

The orientation of the four carbonyls around the W(1) atom and three carbonyls and one SnCl₃ group around the W(2) atom are characterized by their dihedral angles (Table 4).

Tungsten or molybdenum compounds with a 4-3 geometry have not been studied as extensively as the pentagonal bipyramid (PB), capped octahedron (CO) or capped trigonal prism (CTP). The 4-3 geometry is not sufficiently different from the CO and CTP to warrant its inclusion as a separate geometry, particularly for monomers [29,30].

There are four previous structures with which that of 1 might be compared: monomeric $[W(CO)_4Br_3]^-$ anion [28] and dimeric $(\mu\text{-}Cl)_3[Mo(CO)_2L_2]_2^+$ ion, where $L = P(OMe)_3$ [31], $(\mu\text{-}Br)_2[WBr(CO)_4]_2$ and $(\mu\text{-}Br)_3[W_2Br(CO)_7]$ [21]. The closest comparison can be made with the latter. The difference between $(\mu\text{-}Br)_3[W_2Br(CO)_7]$ and the present dimer 1 is that the $SnCl_3^-$ group replaces the Br^-.

The capped octahedral structure has been found for the $[W(CO)_4Br_3]^-$ anion [28]. The structure of $(\mu$-

end, W(2), there are three CO groups and a $SnCl_3^-$ group.

The coordination sphere of each tungsten atom is

Table 3
Anisotropic displacement parameters with e.s.d.s ($\mathring{A}^2 \times 10^3$) [a]

	U_{11}	U_{22}	U_{33}	U_{23}	U_{13}	U_{12}
W(1)	37(1)	22(1)	27(1)	0(1)	1(1)	3(1)
W(1)	31(1)	24(1)	29(1)	1(1)	3(1)	−1(1)
Sn(1)	33(1)	49(1)	36(1)	−2(1)	7(1)	−2(1)
Cl(1)	71(2)	27(2)	38(2)	−3(1)	−9(2)	−13(2)
Cl(2)	90(3)	38(2)	47(2)	11(2)	31(2)	32(2)
Cl(3)	33(2)	79(3)	43(2)	23(2)	−7(2)	−17(2)
Cl(4)	77(3)	75(3)	67(3)	−38(2)	10(2)	9(3)
Cl(5)	40(2)	126(4)	82(3)	−28(3)	−7(2)	−6(3)
Cl(6)	89(4)	116(4)	85(4)	52(3)	42(3)	29(3)
O(1)	105(10)	67(8)	52(7)	−31(6)	23(7)	0(7)
O(2)	54(7)	81(9)	82(9)	36(7)	25(6)	−12(6)
O(3)	137(12)	18(5)	94(9)	4(5)	−9(8)	21(7)
O(4)	52(7)	123(12)	90(10)	16(9)	−30(7)	11(8)
O(5)	65(7)	70(8)	75(8)	18(6)	1(6)	37(7)
O(6)	97(9)	41(7)	98(10)	21(6)	−8(8)	−40(7)
O(7)	80(8)	72(8)	36(6)	−11(5)	−26(6)	−14(6)
C(1)	61(10)	31(8)	50(9)	13(7)	9(7)	0(7)
C(2)	65(10)	39(8)	31(7)	13(6)	3(7)	18(8)
C(3)	77(11)	22(8)	69(10)	−4(7)	0(9)	14(8)
C(4)	50(9)	60(10)	38(8)	−7(7)	−6(7)	−1(8)
C(5)	47(8)	42(8)	28(7)	1(6)	2(6)	5(7)
C(6)	63(9)	43(9)	28(7)	6(6)	−5(6)	−17(7)
C(7)	51(8)	28(7)	61(10)	5(7)	13(8)	−8(7)

[a] Anisotropic vibrational amplitudes in the form $\exp[-2\pi^2(h^2a^{*2}U_{11} + \cdots + 2hka^*b^*U_{12} + \cdots)]$.

Table 4
Dihedral angles (°) in 1 of the type (a) C(n)–W(1)–W(2)–C(m), where $n = 1$–4, and $m = 1$–3 and (b) C(n)–W(1)–W(2)–Sn(1), where $n = 1$–4

| | n | | | |
	1	2	3	4
(a) C(n)–W(1)–W(2)–C(5)	−42.20(11)	44.34(10)	132.01(10)	−134.21(14)
C(n)–W(1)–W(2)–C(6)	49.28(13)	135.82(13)	−136.51(14)	−42.72(18)
C(n)–W(1)–W(2)–C(7)	−140.79(10)	−54.25(11)	33.42(13)	127.20(12)
(b) C(n)–W(1)–W(2)–Sn(1)	131.93(11)	−141.53(10)	−53.86(10)	39.93(12)

Br)$_2$[WBr(CO)$_4$]$_2$ [21] may be described as a two edge-sharing capped octahedra having C_{3v} symmetry about each metal center. Exactly the same 4-3 arrangement about each metal atom as in 1 has been observed only in the $(\mu\text{-Cl})_3$[Mo(CO)$_2$L$_2$]$_2^+$ ion, [31], and $(\mu$-Br)$_3$[W$_2$]Br(CO)$_7$] [21].

The average Cl–Mo–Cl angle 76° in $(\mu\text{-Cl})_3$-[Mo(CO)$_2$L$_2$]$_2^+$ [31] and the mean Br–W–Br angle 78.7° in $(\mu\text{-Br})_3$[W$_2$Br(CO)$_7$] [21] is within the range 76.5° found for Cl–W–Cl in 1. The [W$_2$Br$_9$]$^{2-}$ [32] and [W$_2$Cl$_9$]$^{3-}$ [33] ions also contain a set of three bridging halide atoms, but differ considerably with W–X–W angles 97.1° and 98°, respectively, which is very sensitive to the nature of the W–W bonding. In [W$_2$Br$_9$]$^{-2}$ and [W$_2$Cl$_9$]$^{3-}$, W–W distances are very short, 2.60 and 2.41 Å, respectively. The Cl–W–Cl (ca. 76.5°) and W–Cl–W angles (ca. 88.9°) ensure that there is no metal–metal bonding in 1, the W ··· W contact being

Table 5
Crystal data and details of refinement

Chemical formula	C$_7$Cl$_6$O$_7$SnW$_2$
Molecular weight	895.16
Crystal system	Orthorhombic
Space group	*Pbca*
Cell constants	
a (Å)	12.706(3)
b (Å)	16.655(4)
c (Å)	18.669(3)
V (Å^3)	3951(2)
Z	8
T (K)	293(2)
$F(000)$	3184
D_c (mg m^{-3})	3.010
Radiation λ (Mo Kα) (Å)	0.71069
μ (cm^{-1})	13.706
Crystal size (mm)	0.22×0.30×0.37
Method of collection	$\omega/2\theta$ scan
Reflections determining lattice	25
2θ range (°)	$22.5 < 2\theta < 26.8$
2θ limit (°)	4.0–52.0
No. of reflections	
Collected	3890
Observed, $I > 3\sigma(I)$	2187
Absorptions correction	
μ_{min}, μ_{max}	0.540, 1.886
Residuals R_1, wR_2	0.0299, 0.0746
Final $(\Delta\rho)$ (e Å^{-3})	−0.897/0.787

3.525(1) Å. This is similar to Mo ··· Mo contact of 3.575 Å in the $(\mu\text{-Cl})_3$[Mo(CO)$_2$L$_2$]$_2^+$ ion [31].

The substitution with different terminal ligands (four CO groups or three CO groups and one SnCl$_3^-$ group, respectively) causes the bonding of the bridging ligands between the tungsten atoms to be unsymmetrical; this can be clearly recognized from the W–Cl distances (Table 1). The bridging Cl atoms is slightly closer to W(1) than to W(2). The average W(1)–Cl and W(2)–Cl bond lengths are 2.506(3) Å and 2.530(3) Å, respectively.

The imbalance in the distribution of terminal ligands would, by itself, tend to make W(2) effectively more oxidized than W(1). This is apparent in the shortening of W(2)–CO bond lengths (mean 2.00(1) Å) in comparison to W(1)–CO bonds (mean 2.04(2) Å).

The tungsten–tin bond is short at 2.731(1) Å; the sum of the covalent radii for the two atoms gives 2.97 Å. Semion et al. [34] estimated a covalent radius for tungsten of 1.58 Å, O'Connor and Corey [35] gave 1.39 Å for tin. W–Sn distances of 2.759(3) Å [12a], 2.711(1) Å and 2.737(1) Å [36] have been observed previously. The magnitude of the decrease does suggest a bond order greater than that of the SnCl$_3$ group; it seems probable that the bond does possess some double-bond character [37,38].

In 1, the tin atom is four-coordinate with a geometry that is best described as distorted tetrahedral; the mean W(2)–Sn–Cl angle (116.1°) is greater than the mean Cl–Sn–Cl angle (102.0°), which is consistent with Bent's rule [39] that atomic p character concentrates in orbitals directed towards electronegative substituents. The Sn–Cl distances in 1 (2.314(4), 2.327(4), 2.330(5) Å) show no significant differences but are much more shorter than in uncoordinated trichlorostannate: ca. 2.56 Å in (NH$_4$)$_2$SnCl$_3$Cl(H$_2$O) or ca. 2.53 Å in Cs-SnCl$_3$ [25]. This can be explained by coordination of the trichlorostannate to tungsten which removes electron density from tin. This loss of electron density is compensated by π bonding between the tin and the chloride, thus shortening the tin–chlorine bond [35,36].

2.3. Reaction of [(CO)$_4$W(μ-Cl)$_3$W(SnCl$_3$)(CO)$_3$] (1)

Compound 1 is an excellent starting material for compounds of the form [WCl(SnCl$_3$) (CO)$_3$L$_2$] and

[WCl$_2$(CO)$_3$L$_2$], with L-acetonitrile, phosphine, bipyridine, etc. which are formed according to Eq. (6):

$$[(CO)_4W(\mu\text{-}Cl)_3W(SnCl_3)(CO)_3]$$

$$+ 4L \xrightarrow[\text{Toluene or CH}_2\text{Cl}_2]{\text{Room temperature}} [WCl(SnCl_3)(CO)_3L_2]$$

$$+ [WCl_2(CO)_3L_2] \qquad (6)$$
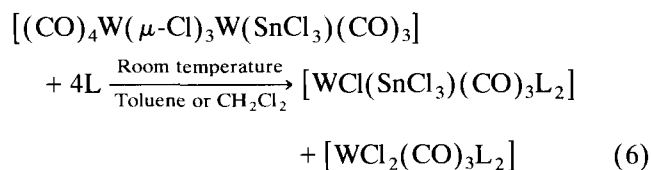
The full characterization of Eq. (6) is being prepared for publication [7]. A similar reaction of 1 with alkynes gives a 1:1 mixture of [WCl$_2$(CO)(RC≡CR')$_2$] and WCl(SnCl$_3$)(CO)(RC≡CR')$_2$] [7].

3. Experimental details

All the reactions were carried out under nitrogen by standard Schlenk line techniques. Solvents applied were dried, distilled and deoxygenated.

The photochemical reactions were carried out in a glass reactor with a quartz window. An HBO 200 mercury lamp was used as the light source. Infrared spectra were recorded with Specord 80 IR and Nicolet FT-IR Model-400 instruments. ^{1}H and ^{13}C NMR spectra were recorded on an AMX 300 Brucker spectrometer. The UV-visible absorption spectra were recorded with a Hewlett Packard 8452A spectrophotometer.

3.1. Preparation of [(CO)$_4$W(μ-Cl)$_3$W(SnCl$_3$)(CO)$_3$] (1)

W(CO)$_6$ (1.0 g, 2.8 mmol) was dissolved in C$_6$H$_{12}$ (100 cm^3) and SnCl$_4$ (0.7 g, 2.8 mmol) was added with continuous stirring under a stream of a nitrogen. The solution was irradiated for 2 h. The IR spectrum of the reaction mixture showed a decay of the absorption due to W(CO)$_6$ accompanied by the appearance of very low intensity new absorption at 2100, 2020, 1942(broad) 1924sh, 1910sh cm^{-1}. An amorphous, orange precipitate was formed. This was filtered off, washed twice with 20 cm^3 C$_6$H$_{12}$ and dissolved in toluene to remove traces of blue decarbonylation product. The solvent was evaporated in vacuo to give an orange residue, which was recrystallized from toluene/heptane to produce an orange microcrystalline solid (yield = 1.15 g, 92%).

Anal. Calc. for C$_7$CL$_6$O$_7$SnW$_2$ C, 9.39; Cl, 23.76; Sn, 13.25%, MW 895.16. Found: C, 9.89; Cl, 23.50; Sn, 13.75%.

Mass spectrum: under standard conditions (electron impact and evaporation from a crucible, the compound decomposes). The main products of thermolysis were [W(CO)$_6$]$^+$ −352 and [SnCl$_2$]$^+$ −190. Other peaks show very low absolute intensities from which only [W(SnCl$_2$)(OH)(CO)$_3$]$^+$ −475 can be identified without doubt. A soft ionization method such as fast atom

bombardment in sulfolane S as matrix material shows a reaction product of S with compound 1, that is [SnClS]$^+$ −275, [WCl(CO)$_2$S]$^+$ −395, [WCl(CO)$_3$S]$^+$ −423, [WCl(CO)$_4$S]$^+$ −451, [WCl(CO)$_2$S$_2$]$^+$ −517, [WCl(CO)$_4$S$_2$]$^+$ −571.

IR(KBr): ν(CO) 2100m, 2020vs, 1990s and 1942s(broad) with shoulders at 1924 and 1910 cm^{-1}; (Nujol) ν(SnCl) 348s, 288w cm^{-1}.

Abs. max. (toluene): λ, nm (ϵ, M^{-1} cm^{-1}): 396(1477), 360(2045), 334(2840), 322(2861), 290(4053).

^{13}C NMR (C$_6$D$_5$CD$_3$): δ (ppm) at 293 K one broad singlet at 204.23 ppm, at 243, 223, 203 and 183 K three signal at 215.43, 209.60 and 204.23 ppm (J^{183}W–^{13}C = 108 Hz). The intensity ratio of carbon CO signals at 243 K is 2:1:4 but changes upon cooling.

3.2. Crystal structure analysis of [(CO)$_4$W(μ-Cl)$_3$-W(SnCl$_3$)(CO)$_3$] (1)

Crystals suitable for X-ray analysis were grown by slow diffusion of heptane into a concentration solution of compound 1 in toluene at ca. 0°C. The single crystal used for the X-ray examination was removed from the flask, rapidly coated with a light hydrocarbon oil to protect it from the atmosphere and sealed in a capillary. Crystallographic data were obtained using KM4 κ-axis computer-controlled [40] four-circle diffractometer with graphite-monochromated Mo Kα radiation. The details of the crystal data intensity measurements are given in Table 5.

The structure was solved by the heavy atom method using the SHELXS-86 program [41] and refined by full-matrix least-squares method, using the SHELXL program [42]. After isotropic refinement, an empirical absorption correction was applied using the program DIFABS [43]. Refinement with anisotropic temperature factors converged to $R_1 = 0.0299$ and $wR_2 = 0.0746$. The final atomic position is given in Table 3. The thermal motion parameters are listed in Table 5. Neutral atomic scattering factors were taken from the International Tables for X-ray Crystallography [44].

References

[1] D. Borowczak, T. Szymańska-Buzar and J.J. Ziólkowski, J. Mol. Catal., 27 (1984) 355.

[2] T. Szymańska-Buzar, *J. Mol. Catal.*, *43* (1987) 161.
[3] T. Szymańska-Buzar, *J. Mol. Catal.*, *48* (1988) 43.
[4] T. Szymańska-Buzar, *J. Mol. Catal.*, *68* (1991) 177.
[5] T. Szymańska-Buzar, *J. Mol. Catal.*, *93* (1994) 137.
[6] S.B. Butts, S.H. Strauss, E.M. Holt, R.E. Stimson, N.W. Alcock and D.F. Shriver, *J. Am. Chem. Soc.*, *102* (1980) 5093.
[7] T. Szymańska-Buzar, unpublished.
[8] T. Szymańska-Buzar, *Inorg. Chim. Acta*, *145* (1988) 231.
[9] T. Szymańska-Buzar, *J. Organomet. Chem.*, *375* (1989) 85.
[10] R. Kummer and W.A.G. Graham, *Inorg. Chem.*, *7* (1968) 310.
[11] K. Edgar, B.F. Johnson, J. Lewis and S.B. Wild, *J. Chem. Soc. (A)*, (1968) 2851.
[12] (a) M. Elder and D. Hall, *Inorg. Chem.*, *8* (1969) 1268; (b) *Inorg. Chem.*, *8* (1969) 1273.
[13] M. Iglesias, A. Lorente, C. DEL Pino and A. Santos, *J. Organomet. Chem.*, *256* (1983) 75.
[14] M. Panizo and M. Cano, *J. Organomet. Chem.*, *287* (1985) 221.
[15] A. Bell and R. Walton, *J. Organomet. Chem.*, *290* (1985) 341.
[16] P.K. Baker and A. Bury, *J. Organomet. Chem.*, *359* (1989) 189.
[17] P.K. Baker and A.J. Quinlan, *Inorg. Chim. Acta*, *162* (1989) 1
[18] D. Miguel, J.A. Perez-Martinez and V. Riera, *J. Organomet. Chem.*, *455* (1993) 121.
[19] M. Cano, M. Panizo, J.A. Campo, J. Tornero and N. Menéndez, *J. Organomet. Chem.*, *463* (1993) 121.
[20] J.A. Bowden and R. Colton, *Aust. J. Chem.*, *21* (1968) 2657.
[21] F.A. Cotton, L.R. Falvello, J.H. Meadows, *Inorg. Chem.*, (1985) 514.
[22] I. Wharf and D.F. Shriver, *Inorg. Chem.*, (1969) 915.
[23] R.J. Clark, L. Maresca and P.J. Smith, *J. Chem. Soc. (A)*, (1970) 2687.
[24] K. Nakamoto, *Infrared and Raman Spectra of Inorganic and Coordination Compounds*, Wiley/Interscience, New York, 1970.

[25] P.G. Harrison, B.J. Haylett and T.J. King, *Inorg. Chim. Acta.*, *75* (1983) 265.
[26] R.J. Ziegler and W.M. Risen, *Inorg Chem.*, *11* (1972) 2796.
[27] R. Colton and J. Kevekordes, *Aust. J. Chem.*, *35* (1982) 895.
[28] M.G.B. Drew and A.P. Wolters, *J. Chem. Soc. Chem. Commun.*, (1972) 457.
[29] M.G.B. Drew, *Prog. Inorg. Chem.*, *23* (1977) 67.
[30] M. Melnik, P. Sharrock, *Coord. Chem. Rev.*, *65* (1985) 49.
[31] M.G.B. Drew, J.D. Wilkins, *J. Chem. Soc., Dalton Trans.*, (1975) 1984.
[32] J.L. Templeton, R.A. Jacobson and R.E. McCarley *Inorg. Chem.*, *16* (1977) 3320.
[33] W.H. Watson Jr. and J. Waser, *Acta Crystallogr.*, *11* (1958) 689.
[34] V.A. Semion, Y.A. Chapovskii, Yu.T. Struchkov and A.N. Nesmeyanov, *Chem. Commun.*, (1968) 666.
[35] J.E. O'Connor and E.R. Corey, *J. Am. Chem. Soc.*, *89* (1967) 3930.
[36] A.L. Balch and D.E. Oram *Organometallics*, *7* (1988) 155.
[37] W. Petz, *Chem. Rev.*, *86* (1986) 1019.
[38] M.S. Holt, W.L. Wilson and J.H. Nelson, *Chem. Rev.*, *89* (1989) 11.
[39] H.A. Bent, *Chem. Rev.*, *61* (1961) 275.
[40] Kuma Diffraction, Kuma KM4 software. User's Guide, version 3.1. Kuma Diffraction, Wroclaw, Poland, 1989.
[41] G.M. Sheldrick, *Acta Crystallogr., Sect. A*, *46* (1990) 467.
[42] G.M. Sheldrick, *J. Appl. Crystallogr.*, in press.
[43] N. Walker and D. Stuart, *Acta Crystallogr., Sect. A*, *39* (1983) 158.
[44] *International Tables for X-ray Crystallography*, Vol. C, Kluwer, Dordrecht, 1992.
[45] C.K. Johnson, ORTEP II, *Report ORNL-5138*, Oak Ridge National Laboratory, Tennessee, USA, 1976.